ELSEVIER

Nuclear Instruments and Methods in Physics Research B 96 (1995) 7–12

NIM B
Beam Interactions with Materials & Atoms

Negative-ion implantation technique

Junzo Ishikawa [a,*], Hiroshi Tsuji [a], Yoshitaka Toyota [a], Yasuhito Gotoh [a], Koji Matsuda [a], Masayasu Tanjyo [b], Shigeki Sakai [b]

[a] *Department of Electronics, Kyoto University, Yoshida-honmachi, Sakyo-ku, Kyoto 606-01, Japan*
[b] *R&D Division, Nissin Electric Co., Ltd., 575 Kuze-Tonoshiro, Minami-ku, Kyoto 601, Japan*

Abstract

Negative-ion implantation is a promising technique for charging-free implantation for the forthcoming ULSI fabrication, in which the wafer charging by positive-ion implantation will become a troublesome problem even with an electron shower. The negative-ion implantation technique remarkably ameliorates such a charging problem since the incoming negative charge of implanted negative ions is easily balanced by the outgoing negative charge of a part of secondary electrons. Thus, the surface charging voltage is maintained to within about ± 10 V for isolated conducting materials and insulators, and is free from space and time fluctuations. A high-current negative-ion source and a medium current negative-ion implanter developed for this technique are described with the design concepts. In addition, the fundamental measurements of interactions between the negative-ion beam and the gas/solid are also described.

1. Introduction

It has long been believed that positive ions are more easily produced in comparison with negative ions and that the effects of negative ions on a solid surface are almost the same as those of positive ions. Thus, positive ions have been used in the conventional ion implantation technique. Recent progress in negative-ion technology for materials science [1–3], however, has attracted a great deal of attention with the discovery of new phenomena in negative-ion beam/solid surface interaction, as well as the development of high current heavy negative-ion sources. Especially when negative ions are used in ion implantation into insulated materials, the surface charging voltage is found to be quite low [2,3]. Therefore, negative-ion implantation is expected to be a promising technique as a charging-free ion implantation method for the forthcoming ULSI (more than 256 Mbits) fabrication processes.

For industrial application of negative-ion implantation, an RF-plasma-sputter-type heavy negative-ion source [4,5] and a medium current negative-ion implanter have been developed, based on the measurements of negative-ion production probabilities [6–8] and electron detachment cross-sections [9,10]. In addition, fundamental phenomena related to negative-ion implantation, such as secondary electron emission factors [1], implanted depth profiles of negative ions [1,11], charging due to negative-ion implantation [2,3,12] etc., have been revealed.

2. Production and electron detachment of negative ions

2.1. Negative-ion production probability [6–8]

Heavy negative-ion production by sputtering a solid surface with a low work function, i.e., secondary negative-ion emission by sputtering, is quite effective. When a sputtered atom leaves a metal surface, the atom can easily obtain an electron for its electron affinity level from the surface, due to a lowering and broadening effect of the affinity level. The negative-ion production probabilities were measured for various kinds of heavy elements when a cesiated solid surface was sputtered by xenon ions [6–8]. The maximum production probabilities for typical heavy elements are listed in Table 1, and they show high values of about 10%. The probability can be expressed by the following semi-empirical equation [8].

$$P^-(v) = \frac{2}{\pi}\exp\left[-\frac{\phi_{\min} - E_a}{2a_0 v \cos\theta/\pi + kT_{\text{eff}}}\right], \quad (1)$$

$$a_0 = 2.0\times 10^{-5}\ [\text{eV s/m}],$$

$$kT_{\text{eff}} = 0.073 + 2.0\times 10^{-3}\ M\ [\text{eV}], \quad (2)$$

where a_0 is the decaying factor and T_{eff} is the local effective temperature of the surface on ion bombardment, v and θ are the ejecting velocity and angle, respectively,

* Corresponding author. Tel. +81 75 753 5325, fax +81 75 751 0297.

0168-583X/95/$09.50
SSDI 0168-583X(94)00444-7

Table 1
Maximum negative-ion production probabilities due to secondary negative-ion emission by sputtering

	Negative ion				
	C	Si	Cu	Ge	W
Probability [%]	18.3	15.6	12.1	13.6	8.1

of the sputtered particle from the surface, ϕ_{min} is the minimum work function of the surface, and E_a and M are the electron affinity and atomic mass number of the sputtered particles, respectively.

Therefore, secondary negative-ion emission by sputtering can be used as an ion-production mechanism of high current heavy negative-ions [4,5,13–16].

2.2. Electron detachment cross-sections [9,10]

A negative ion easily releases an attached electron and becomes a neutral atom when colliding with gas particles. The survival negative-ion current, $I(n_0L)$, after passing through a distance L with a gas density of n_0, is estimated from single- and double-electron detachment cross-sections (σ_{-10} and σ_{-11}), as shown below:

$$I(n_0L) = I_0 \exp[-(\sigma_{-10} + \sigma_{-11})n_0L]. \quad (3)$$

When a plasma-sputter type heavy negative-ion source is used, the residual gas in the ion beam transport region is mainly xenon. The single- and double-electron detachment cross-sections for various kinds of negative ions, using a xenon gas target, were measured [9,10] as shown in Fig. 1. In the ion energy range of 5–40 keV, σ_{-10} is almost constant in the order of 10^{-15} cm^2, while σ_{-11} ranges between 10^{-17}–10^{-16} cm^2. Thus, the residual xenon gas pressure in the negative-ion beam transport region (assuming a distance of several meters) should be lower than

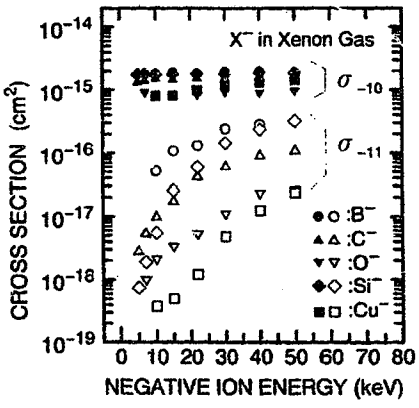

Fig. 1. Single- and double-electron detachment cross-sections for various kinds of negative ions using a xenon gas target.

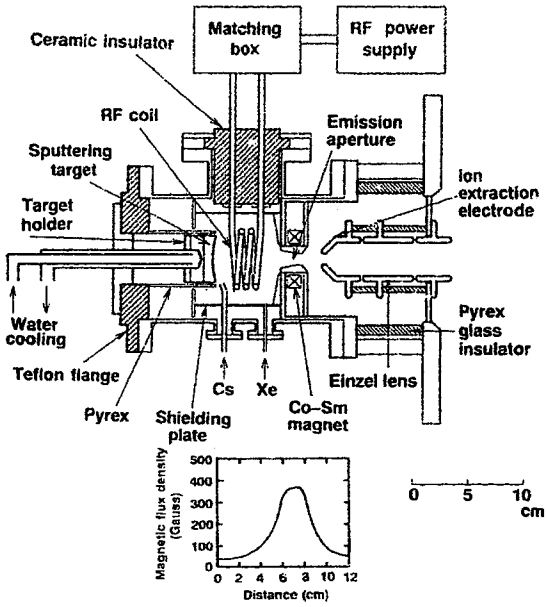

Fig. 2. Schematic diagram of an RF-plasma-sputter-type heavy negative-ion source.

10^{-6} Torr in order to obtain a survival negative-ion current of more than 90%.

3. Negative-ion source and negative-ion implanter

3.1. DC high current heavy negative-ion source [4,5]

In order to obtain DC high-current negative ions in secondary negative-ion emission by plasma-sputtering of a cesiated target surface, the following conditions are required: a large sputtering target surface, uniform sputtering by plasma ions, a precise cesium supply to the sputtering target, temperature control of the sputtering target, and a low gas pressure discharge.

Based on these concepts, an RF-plasma-sputter-type heavy negative-ion source [4,5] was developed as shown in Fig. 2, which can deliver up to 10 mA of various kinds of negative-ion beams. A dense plasma in the order of 10^{11} cm^{-3}, is generated by an RF (13.56 MHz) discharge with an RF coil at a relatively low xenon gas pressure in the order of 10^{-4} Torr. The source had a sputtering target whose diameter was 42 mm. The maximum DC negative-

Table 2
Maximum negative-ion currents extracted from the RF-plasma-sputter-type heavy negative-ion source

	Negative ion					
	B_2^-	C^-	C_2^-	Si^-	P^-	Cu^-
Ion current [mA]	1.0	1.6	2.3	3.8	0.8	12.1

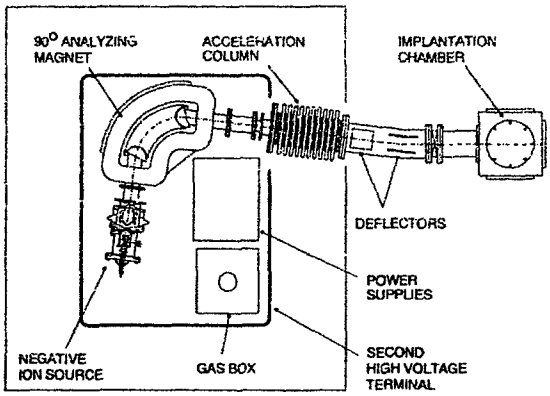

Fig. 3. Schematic configuration of a medium current negative-ion implanter.

ion currents measured just after the extraction electrode were in the order of milliamperes and are listed in Table 2. These are considered to be sufficient for negative-ion implantation into semiconductors.

3.2. Negative-ion implanter

A medium current negative-ion implanter is now being developed so that a milliampere order of negative-ion current can be accelerated up to an energy of more than 100 keV. The schematic configuration of a newly designed negative-ion implanter is shown in Fig. 3. The implanter consists of a negative-ion source (in the second high-voltage terminal), an analyzing magnet with a bending angle of 90° (in the first high-voltage terminal), an acceleration column for acceleration of more than 100 kV, and an implantation chamber. The negative-ion source is a newly designed and small version of an RF-plasma-sputter-type heavy negative-ion source with a sputtering target of 20 mm in diameter and an exit aperture of 5 mm in diameter. Fig. 4 shows a photograph of the source mounted in the high-voltage terminal of the implanter. As for the vacuum pumping system, 6- and 4-in. oil diffusion pumps are used for the evacuation of the ion source and beam transport regions, respectively, and a 6-in. turbo molecular pump is used in the target chamber region. The background and operating (with xenon gas flow of 0.03 ccm) gas pressures are less than 1×10^{-6} and 3×10^{-6} Torr, respectively. In a preliminary experiment, Cu^- of 0.1 mA was obtained at the implantation chamber at an ion-beam energy of 10 keV, where the operating conditions were as follows; 8.3×10^{-5} Torr of Xe gas at the plasma region, 100 W of input RF power, 400 V of sputtering voltage and 12 mA of target current, and 260°C of Cs oven temperature. The implanter has now been tested to obtain the optimum operational conditions.

4. Negative-ion implantation

4.1. Secondary-electron-emission factor induced by negative-ion bombardment

A negative-ion beam is considered to induce more secondary electrons than a positive-ion beam, since a negative ion easily releases an attached electron on bom-

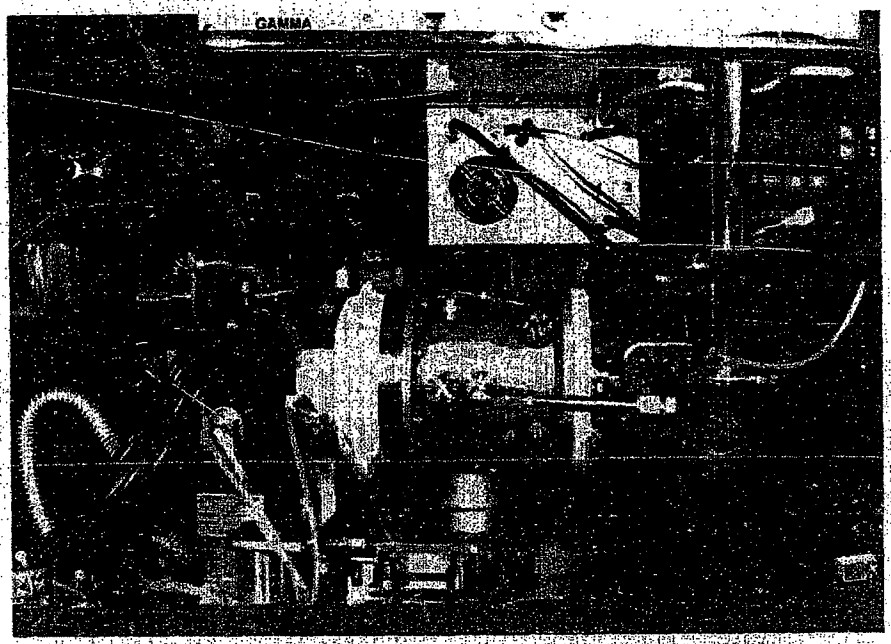

Fig. 4. Photograph of the negative-ion source mounted in the negative-ion implanter.

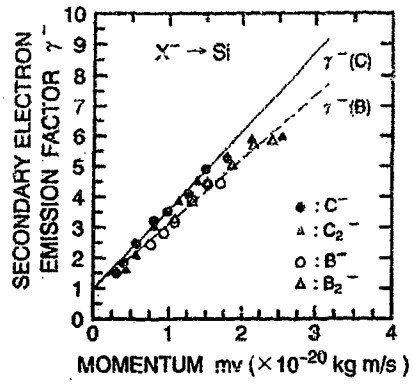

Fig. 5. Secondary-electron-emission factors as a function of the ion momentum of carbon and boron negative-ion beams when bombarding a silicon substrate.

bardment. Fig. 5 shows the secondary-electron-emission factory γ^- as a function of ion momentum for carbon [1] and boron negative-ion beams when negative ions bombard a silicon substrate at a residual gas pressure in the order of 10^{-6} Torr. The value of γ^- should consist of two terms: a constant term due to the detachment of one electron attached to a negative ion and a linear-increase term due to kinetic emission.

4.2. Depth profile of negative-ion implantation into insulators

Fig. 6 shows the depth profile of implanted carbon atoms by C^- implantation into a SiO_2 substrate at an energy of 20 keV with a dose of 1×10^{16} ions/cm^2, which was quantitatively analyzed by SIMS. The measured depth profile coincides well with a theoretical curve calculated by the LSS theory, although in conventional positive-ion implantation, a depth profile of implanted atoms is sometimes quite different from an expected one, due to charging of the implanted insulators.

In addition, cesium atoms were not detected in the implanted layer (noise level by SIMS) as shown in Fig. 6, although cesium vapor was used in the negative-ion source.

4.3. Surface charging voltage of insulated materials by negative-ion implantation

In the LSI fabrication processes, ion implantation into isolated conductive materials (such as poly-silicon and Al electrode) and insulators (such as SiO_2 and photoresist layer), is indispensable. Charging problems on these material surfaces by conventional positive-ion implantation have become extremely severe, even with an electron shower as the design becomes smaller and smaller [17,18].

4.3.1. Negative-ion implantation into isolated conducting materials [2,3,12]

When negative ions are implanted into an isolated conducting material, the surface charging voltage is determined by the balance of incoming negative charge due to negative ions, and outgoing negative charge due to a part of secondary electrons. The outgoing charge is the high energy part of the secondary-electron energy distribution, which has a higher energy than the surface charging voltage. Therefore, the surface charging voltage is increased with an increase in the secondary-electron emission factor since the relative shape of secondary-electron energy distribution is not strongly dependent on parameters such as ion energy and ion species for the same material.

Fig. 7 shows an example of the surface charging voltage of isolated Si substrate (Si substrate on a 1.1 mm thick non-alkaline glass plate) as a function of the ion energy by carbon negative-ion implantation. The surface charging voltage was measured with a high-impedance voltmeter and was a saturated value. The surface charging voltage by

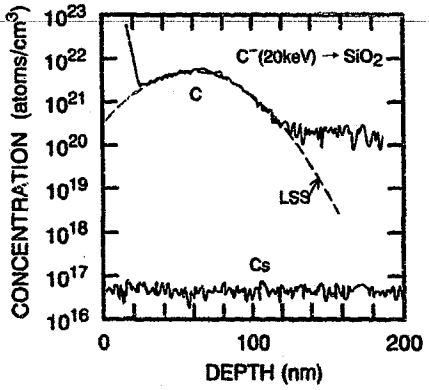

Fig. 6. Depth profile of implanted carbon atoms by C^- implantation into SiO_2 substrate at an energy of 20 keV and a dose of 1×10^{16} ions/cm^2. The profile was quantitatively measured by SIMS. Cs atom signals are at a noise level.

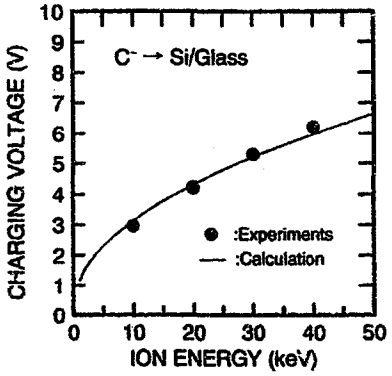

Fig. 7. Surface charging voltage of isolated Si substrate as a function of the ion energy by carbon negative-ion implantation. A theoretically calculated curve is also indicated.

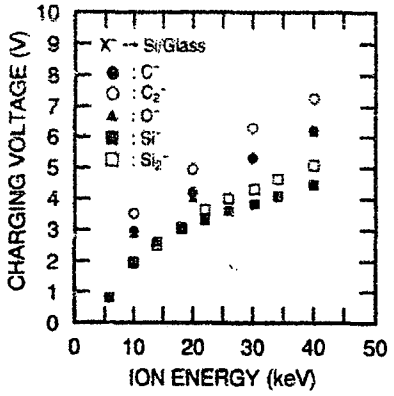

Fig. 8. Surface charging voltages of isolated Si substrate by negative-ion implantation for various negative ions, as a function of the ion energy.

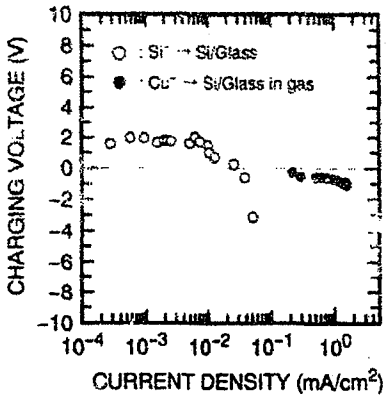

Fig. 9. Dependence of surface charging voltage of isolated Si substrate on the negative-ion current density at an implantation ion energy of 15 keV under a high vacuum condition (○) and a relatively high xenon gas pressure (10^{-4} Torr order) condition (●).

negative-ion implantation was quite low (within several volts), and gradually increased with the ion energy, due to the ion energy dependence of the secondary-electron-emission factor. Assuming that an energy distribution function of the secondary-electron emission is expressed by $f(E) = 4E_pE/(E+2E_p)^3$ ($E_p = 0.34$ eV) and applying the measured secondary-electron-emission factors, an expected charging voltage can be theoretically calculated from the above mentioned charge balance. In Fig. 7, the calculated curve is also indicated by a line, which coincides well with the experimental values. This charge balance on the conducting material surface occurred at the same area and at the same time as negative-ion bombardment, thus the surface charging voltage is free from space and time fluctuations.

Fig. 8 shows the surface charging voltage of isolated Si substrate by negative-ion implantation for various negative ions as a function of the ion energy. Although these charging voltages vary slightly among negative-ion species, depending on the value of their secondary-electron-emission factors, they are within several volts.

Fig. 9 shows the dependence of the surface charging voltage of isolated Si substrate upon the negative-ion current density (beam size of 10 mm in diameter) at an implantation ion-energy of 15 keV under a high vacuum condition and a relatively high xenon gas pressure (10^{-4} Torr order) condition. Under the high vacuum condition, the surface charging voltage showed a positive low value of about 2 V in a current density range below 10 $\mu A/cm^2$. However, it decreased and became negative with an increase in the current density above 10 $\mu A/cm^2$. This is because a beam potential of negative-ions causes a decrease in the surface charging voltage, since the surface charging voltage can be controlled by adjusting the electrode voltage just in front of the surface [2]. On the contrary, under the relatively high gas pressure condition, the surface charging voltage was nearly 0 V even at a high current density of the order of mA/cm^2, since the beam potential effect would be weakened due to charge neutralization of the negative-ion beam.

4.3.2. Negative-ion implantation into insulators

Surface charging voltage of insulators by negative-ion implantation can be evaluated by measuring an energy distribution of secondary electrons emitted from the surface [2], since the peak of the energy distribution is shifted according to the voltage difference between the surface and ground voltages. Fig. 10 shows the energy distributions of secondary electrons from the surface of photoresist (OFPR-800:100 nm on Si substrate), where the distribution peak from an Al plate at the ground voltage is indicated by an arrow as a reference. Each distribution peak from the photoresist surface was shifted to the high energy side by several eV compared with that of the grounded Al plate. Therefore, the surface charging voltage

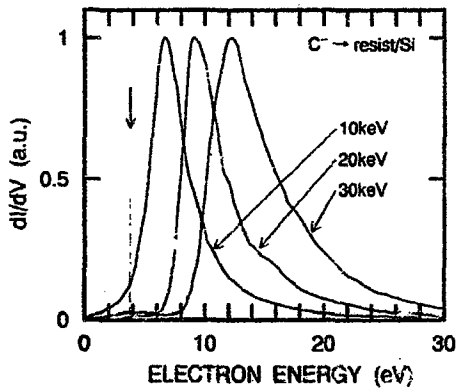

Fig. 10. Secondary-electron energy distribution from the surface of photoresist (OFPR-800) as a parameter of the ion energy of carbon negative-ion implantation. As a reference, the distribution peak voltage from an Al plate at the ground voltage is indicated with an arrow.

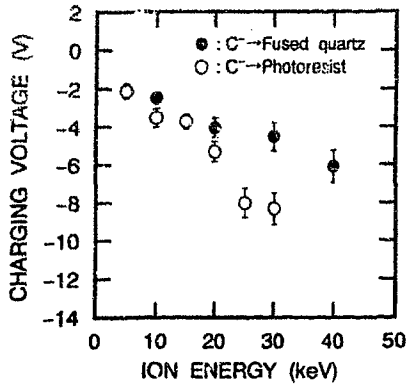

Fig. 11. Surface charging voltage of fused quartz (SiO_2) and photoresist (OFRP-800) as a function of the ion energy by carbon negative-ion implantation.

of insulators is considered to be negative by several volts, the polarity being opposite to that of the isolated conducting materials. The reason for this is not well understood at present. Fig. 11 shows the surface charging voltage of insulators (fused quartz and photoresist) by carbon negative-ion implantation as a function of the ion energy. The surface charging voltage of typical insulators by negative-ion implantation, is within -10 eV.

5. Concluding remarks

Since the RF-plasma-sputter-type heavy negative-ion source delivers DC milliampères class of heavy negative-ion currents, a medium current negative-ion implanter could be nominated as actual surface processing apparatus. The characteristics of surface charging of isolated conducting materials and insulators are advantageous for the forthcoming ULSI fabrication processes, because their surface charging voltages are very low, within ± 10 V so that no breakdown would take place even in extremely thin film insulators of ULSI. In addition, as a whole system, the negative-ion implanter, which need not have any charge neutralizer, is simpler and more economical than conventional positive-ion implanters. Therefore, negative-ion implantation is a promising technique in the future technology.

References

[1] J. Ishikawa, Rev. Sci. Instr. 63 (1992) 2368.
[2] J. Ishikawa, Rev. Sci. Instr. 65 (1994) 1290.
[3] J. Ishikawa, Surf. Coat. Technol. 65 (1994) 64.
[4] J. Ishikawa, H. Tsuji, Y. Okada, M. Shinoda and Y. Gotoh, Vacuum 44 (1993) 207.
[5] H. Tsuji, J. Ishikawa, Y. Gotoh and Y. Okada, Proc. 6th. Int. Symp. on Production and Neutralization of Negative Ions and Beams, Brookhaven, 1992, AIP Conf. Proc. Ser. No. 287 (AIP, New York, 1994) p. 530.
[6] J. Ishikawa, Nucl. Instr. and Meth. B 37/38 (1989) 38.
[7] H. Tsuji and J. Ishikawa, Rev. Sci. Instr. 63 (1992) 2488.
[8] J. Ishikawa, H. Tsuji, Y. Gotoh and S. Azegami, Ref. [5], p. 66.
[9] J. Ishikawa, H. Tsuji and T. Maekawa, Vacuum 39 (1989) 1129.
[10] H. Tsuji, J. Ishikawa, T. Maekawa and T. Takagi, Nucl. Instr. and Meth. B 37/38 (1989) 1127.
[11] J. Ishikawa and H. Tsuji, Nucl. Instr. and Meth. B 74 (1993) 118.
[12] S. Sakai, M. Tanjyo, K. Matsuda, Y. Gotoh, H. Ohnishi, H. Tsuji and J. Ishikawa, Proc. 9th Int. Conf. on Ion Implantation Technology, 1992 (Elsevier, 1993) p. 617.
[13] R. Middleton, Nucl. Instr. and Meth. 118 (1974) 329.
[14] H.H. Anderson and P. Tykesson, IEEE Trans. Nucl. Sci. NS-22 (1975) 16332.
[15] Y. Mori, Rev. Sci. Instr. 63 (1992) 2357.
[16] G.D. Alton, Y. Mori, A. Takagi, A. Ueno and S. Fukumoto, Nucl. Instr. and Meth. A 270 (1988) 194.
[17] M.E. Mack, G. Ryding, D.H. Douglas-Hamilton, K. Steeples, M. Farley, A. Wittkower and R. Lambracht, Nucl. Instr. and Meth. B 6 (1985) 405.
[18] V.K. Basra, C.M. Mckenna and S.B. Felch, Nucl. Instr. and Meth. B 21 (1987) 360.